

Geophysical Research Letters[®]



RESEARCH LETTER

10.1029/2023GL104931

Bin Zhou, Zhe Wang, and Xiangchun Xu are co-first authors of the article.

Key Points:

- Pleistocene temperature, rainfall, and C₄ plants ratios are quantitatively reconstructed from the Shangchen loess deposits with artifacts
- High climate variability, C₄ plants expansion and aridification suspended hominin occupation at Shangchen during the early mid-Pleistocene climate transition
- Hominins responded differently to large-scale climate oscillations depending on distinctive local environmental conditions

Supporting Information:

Supporting Information may be found in the online version of this article.

Correspondence to:

B. Zhou,
zhoubinok@163.com

Citation:

Zhou, B., Wang, Z., Xu, X., Pang, Y., Bird, M. I., Wang, B., et al. (2023). Hominin response to oscillations in climate and local environments during the mid-Pleistocene climate transition in northern China. *Geophysical Research Letters*, 50, e2023GL104931. <https://doi.org/10.1029/2023GL104931>

Received 14 JUN 2023

Accepted 3 OCT 2023





Author Contributions:

Conceptualization: Bin Zhou, Zhe Wang, Xiangchun Xu

Data curation: Zhe Wang, Xiangchun Xu, Yang Pang

Funding acquisition: Bin Wang

Hominin Response to Oscillations in Climate and Local Environments During the Mid-Pleistocene Climate Transition in Northern China

Bin Zhou¹ , Zhe Wang¹ , Xiangchun Xu¹, Yang Pang¹ , Michael I. Bird², Bin Wang³, Michael E. Meadows^{4,5} , and David Taylor⁶

¹Key Laboratory of Surficial Geochemistry (Ministry of Education), School of Earth Sciences and Engineering, Nanjing University, Nanjing, China, ²College of Science and Engineering and ARC Centre of Excellence for Australian Biodiversity and Heritage, James Cook University, Cairns, QLD, Australia, ³National Demonstration Center for Experimental Geography Education, School of Geography and Tourism, Shaanxi Normal University, Xi'an, China, ⁴School of Geography and Ocean Sciences, Nanjing University, Nanjing, China, ⁵Department of Environmental & Geographical Science, University of Cape Town, Cape Town, South Africa, ⁶Department of Geography, Faculty of Arts and Social Sciences, National University of Singapore, Singapore, Singapore

Abstract Archeological evidence from loess sediments from Shangchen on the southeastern Chinese Loess Plateau indicates a suspension of hominin occupation around the time of the early mid-Pleistocene climate transition, prompting a re-assessment of climate-vegetation-hominin interactions. Loess deposits with in situ lithic records cover the period of hominin occupation and reveal four distinct climate-vegetation periods (2.1–1.8, 1.8–1.26, 1.26–0.9, and 0.9–0.6 Ma). Major oscillations in climate superimposed upon an aridification trend and an expansion of C₄ herbaceous vegetation from about 1.26 Ma may have driven early humans to move to more hospitable locations in the region. Comparison with the record at Nihewan indicates that large-scale climate oscillations induced disparate hominin responses due to distinctive local environmental conditions.

Plain Language Summary A combination of several lines of evidence suggests that changes in climate and their impacts on the availability of food and shelter from around 1.26 million years ago may have driven the dispersal of early humans from the southeastern Chinese Loess Plateau to more hospitable environments elsewhere in the region.

1. Introduction

Large-scale shifts in climate and changes in climate variability have been hypothesized to influence human evolution (deMenocal, 2011; Potts, 1996). Sediment records reveal that past periods of profound climate change, such as the mid-Pleistocene climate transition (MPT; typically defined as 1.2–0.7 Ma), exerted a significant influence on early humans in eastern Africa (Maslin et al., 2014). The extent of similarities of the case in East Asia has remained largely unstudied, however, due to the limited hominin record. The extreme rarity of fossilized hominin remains outside Africa, and lack of studies investigating the impact of local environmental conditions on hominin habitation, dispersal and evolution (Blumenthal et al., 2017; Magill et al., 2013a, 2013b; Owen et al., 2018; Potts et al., 2020; Yang et al., 2021), has hindered any evaluation of the relationship between environmental factors and hominin activities. This imbalance has been redressed, somewhat, through the discovery of a *Homo erectus* cranium (1.63–1.62 Ma) at Gongwangling (Zhu et al., 2015) and a *H. erectus* mandible (~0.65 Ma) at Chenjiawo (An & Ho, 1989), in the southeastern part of the Chinese Loess Plateau (CLP), and the subsequent investigation of more than 40 Pleistocene-age paleolithic sites in the region (S. Wang et al., 2014). More recently, a sequence of loess-paleosol deposits that includes paleolithic artifacts, as Zhu et al. (2018) rule out the possibility of a natural origin, has been discovered at Shangchen (Zhu et al., 2018), around 4 km north of Gongwangling (Figure 1), providing the earliest evidence for hominin occupation outside Africa (oldest to ~2.1 Ma). However, the stone tool record indicates that this occupation was interrupted around the time of the onset of the MPT (layer L15, dated ca. 1.26 Ma; Zhu et al., 2018).

Thick eolian loess-paleosol sequences of the CLP have yielded virtually continuous long records of climate and vegetation change during and since the Miocene (An et al., 2005; Z. Guo et al., 2002). Our understanding of environmental change on the CLP is based upon an expanding range of sediment-based evidence, including

© 2023. The Authors.

This is an open access article under the terms of the [Creative Commons Attribution-NonCommercial-NoDerivs License](https://creativecommons.org/licenses/by-nc-nd/4.0/), which permits use and distribution in any medium, provided the original work is properly cited, the use is non-commercial and no modifications or adaptations are made.

Investigation: Bin Zhou, Zhe Wang, Xiangchun Xu, Yang Pang, Michael I. Bird, Bin Wang, Michael E. Meadows, David Taylor

Methodology: Bin Zhou, Zhe Wang, Xiangchun Xu, Yang Pang, Bin Wang

Software: Zhe Wang

Validation: Bin Zhou, Zhe Wang, Xiangchun Xu

Visualization: Bin Zhou, Zhe Wang, Xiangchun Xu, Yang Pang, Bin Wang

Writing – original draft: Bin Zhou, Xiangchun Xu

Writing – review & editing: Bin Zhou, Zhe Wang, Xiangchun Xu, Michael I. Bird, Michael E. Meadows, David Taylor

traditional proxies of magnetic susceptibility (SUS; An et al., 2005), total organic carbon content (TOC%) and its associated carbon isotope composition ($\delta^{13}\text{C}_{\text{TOC}}$; Chen et al., 2006), pollen (Wu et al., 2007) and black carbon content (BC%; Zhou et al., 2007, 2014), etc., as well as novel proxies such as branched glycerol dialkyl glycerol tetraethers (br-GDGTs; Peterse et al., 2014). Here, we present new data on br-GDGTs, SUS, TOC%, $\delta^{13}\text{C}_{\text{TOC}}$, and %BC from sequences of loess and paleosol deposits that accumulated from 2.1 to 0.6 Ma in order to: (a) reconstruct the trajectory and variability in environmental conditions at/around Shangchen using organic geochemical proxies; (b) compare paleoenvironmental variations with the artifact record to explore the relationship between local environmental conditions and hominin occupation of the site; and (c) investigate the primary factors in hominin choice of habitats in northern China, East Asia.

2. Materials and Proxies

2.1. Sampling and Age Model

Shangchen (34°13'33"N, 109°28'39"E), and Duanjiapo (34°11'15"N, 109°13'58"E) are both located in Lantian County, Shaanxi Province (12), with elevations ranging from 420 to 2,449 m above sea level (Figure 1 and Supporting Information S1). Loess (L) and paleosol (S) samples were collected from the S27 paleosol layer to the L6 loess layer at Shangchen, corresponding to ~2.1 to ~0.6 Ma, with a total of 48 samples selected with one sample from each single loess or paleosol strata for measuring SUS, TOC%, $\delta^{13}\text{C}_{\text{TOC}}$, and %BC. A total of 24 samples from L6, L9, L13, S14, L15, S15, L22, S22, L25, S25, L26, and S26 were selected for measuring br-GDGTs at Shangchen and Duanjiapo, respectively.

Zhu et al. (2018) linked five subsections with artifacts excavated to establish the precise magnetostratigraphy at Shangchen locality (Supporting Information S1), with the oldest artifact dating to ca. 2.12 Ma. The age model of our data is based on the Chiloparts timescale (Ding et al., 2002; Zhu et al., 2018), which correlates with the paleomagnetic timescale of Shangchen section (Zhu et al., 2018; Text S1 in Supporting Information S1). It is also supported by $^{26}\text{Al}/^{10}\text{Be}$ burial ages from other sections around this area (Shen et al., 2020; Y. Sun et al., 2019; Tu et al., 2017; Text S1 and Figure S2 in Supporting Information S1).

2.2. Proxies

Proxies were selected that have previously proved to be effective in reconstructing paleoclimate and paleovegetation history on the CLP. Magnetic SUS is widely accepted as a proxy for the East Asian Monsoon (An et al., 2005). Despite the potential minor inputs of carbon from microbial and aeolian sources, the stable carbon isotope composition of total organic matter in soil ($\delta^{13}\text{C}_{\text{TOC}}$) can be used as a direct indicator of the distribution and relative abundance of C_3 (including trees, shrubs and grasses) and C_4 (mainly warm and/or arid climate herbaceous) plants in the vegetation (Liu et al., 2005; Zhou et al., 2016). BC is a term synonymous with pyrogenic carbonaceous materials, or pyrogenic carbon, which originates from the combustion of biomass, including fossil fuels (Bird et al., 2015). The amount of BC (%BC) in sediment samples has been used as a proxy for the incidence and extent of burning of local vegetation, with elevated values indicating a trend toward aridification (Han et al., 2020; Zhou et al., 2014). The molecular structure of cell membranes of living br-GDGTs-producing soil microbes (bacteria) varies with environmental conditions, notably air temperature and soil pH, which has allowed br-GDGTs to be used in reconstructing variations in mean annual temperature of land surface (MAT) and precipitation (MAP) over extended periods of time (Peterse et al., 2014; Weijers et al., 2007).

The pre-treatment process, instrumental analysis and data processing of each proxy is presented in Text S2 in Supporting Information S1.

3. Results

3.1. Magnetic Susceptibility

The samples used in this study are from the same batch as those for which there is already precise chronological control derived from paleomagnetic dating (Zhu et al., 2018). We re-measured the SUS of the samples (Figure 2a) with results that are in close accord with those previously published in Zhu et al. (2018) (Figure S3 in Supporting Information S1). As is the case elsewhere on the CLP, SUS exhibits substantial changes across the early MPT,

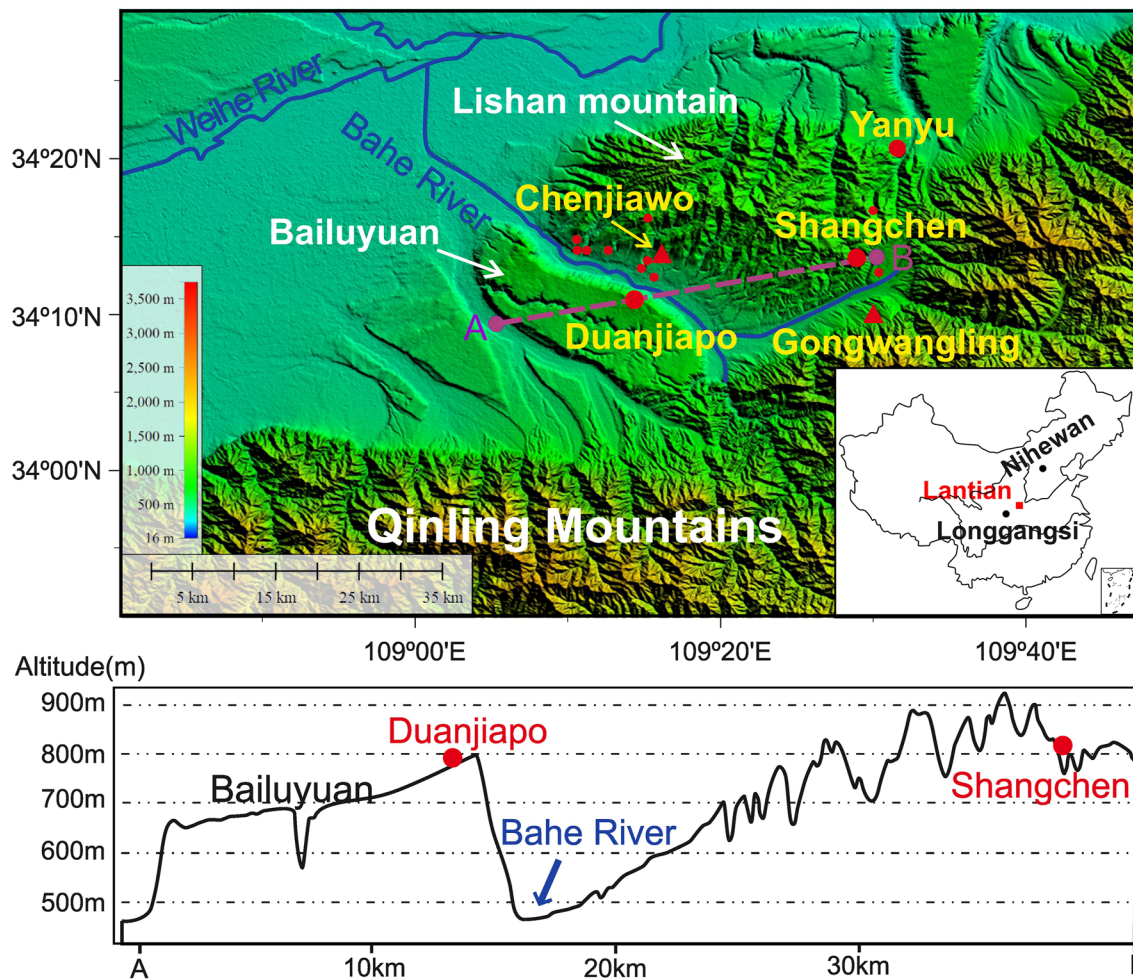


Figure 1. Study area. Shangchen is located at Lantian in the southeast of Chinese Loess Plateau and the north of the Qinling Mountains. Bailuyuan tableland is a flat loess tableland. Red large dots: study sites. Red small dots: paleolithic sites. Red triangles: locations of major hominin sites in the Lantian area. Lower figure shows variations in elevation along the transect between A and B, and two study sites mentioned in the text, Duanjiapo and Shangchen. The localities of Lantian, Longgangsi, and Nihewan referred to in this paper are shown in the inset map.

between ca. 1.26 Ma and ca. 0.9 Ma (Song et al., 2014), when climate oscillations switched from being mostly symmetrical, with a periodicity of about 41-Kyr, to being markedly asymmetrical, with 100-Kyr cycles (Willeit et al., 2019).

3.2. Total Organic Carbon (%TOC) and BC (%BC)

The concentration of TOC across all samples ranges from 0.05% to 0.17% (mean = 0.10%, $n = 48$) and exhibits a trend of increasing values through the sequence (Figure 2b). %BC varies from 0.06‰ to 0.19‰ (mean = 0.1‰, $n = 48$), with increasing concentrations from about L15 (~1.26–1.24 Ma; Figure 2c). Percentages of both TOC and BC differ markedly between glacial and interglacial periods during 1.26–0.9 Ma, with lower values in loess layers and higher values in paleosol layers (Figures 2b and 2c).

3.3. $\delta^{13}\text{C}_{\text{TOC}}$

$\delta^{13}\text{C}_{\text{TOC}}$ ($n = 48$) ranges from -23.15‰ to -27.23‰ , with values in loess being generally more depleted than in the paleosols (t -value = -2.58 , $p = 0.013$, <0.05 , Figure 2d). Mass balance calculations show that C_4 taxa account for less than 30% of the biomass throughout the entire period represented by the sequence of samples analyzed (Figure 2d). From L25 to S15 (~1.8–1.26 Ma), more depleted $\delta^{13}\text{C}_{\text{TOC}}$ indicates the predominance of C_3 plants. The contribution from C_4 taxa increased at S15 (~1.28 Ma) and especially between S11–L9 (~1.15–0.9 Ma).

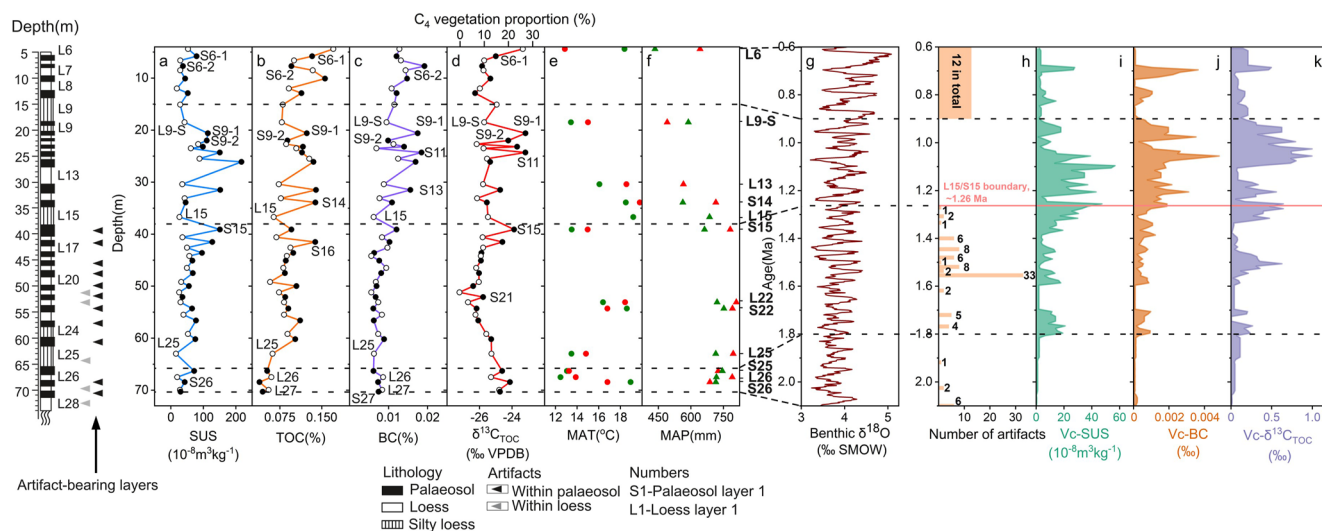


Figure 2. Stratigraphy of the Shangchen section and sequences of proxies from both the Shangchen and Duanjiapo sections. (a) Magnetic susceptibility data from Shangchen: higher values are evident in paleosol layers (S, solid circles) while lower values are evident in loess layers (L, hollow circles). (b) Total organic carbon (TOC%). (c) Black carbon (BC%). (d) $\delta^{13}\text{C}_{\text{TOC}}$ at Shangchen. Equations in G. Wang et al. (2008) and Yang et al. (2015) have been used to determine proportions of C_4 plants. (e) Mean annual temperature (MAT): green circles represent Shangchen by depth, and red circles represent Duanjiapo by layers. (f) Mean annual precipitation (MAP): green triangles represent Shangchen by depth, and red triangles represent Duanjiapo by layers. (g) Benthic $\delta^{18}\text{O}$ stack (Lisiecki & Raymo, 2005). (h) Timeseries of number of artifacts excavated at Shangchen. Each column represents a layer from the loess-paleosol sequence. (i–k) Variability changes of climatic and environmental proxies. Red solid line represents L15/S15 boundary.

3.4. br-GDGTs

Wide ranges of br-GDGTs-derived land surface MAT are evident at Shangchen and Duanjiapo, with similar mean values of 16.0°C ($12.5\text{--}19.2^\circ\text{C}$, $n = 12$) and 15.9°C ($12.9\text{--}19.8^\circ\text{C}$, $n = 11$), respectively. Variations in br-GDGTs-derived MAT are consistent with estimated and modeled continental MAT at 36°N (Figure S5 in Supporting Information S1). Surface MAT is shown to have fluctuated between 2.1 and 0.6 Ma, with sharp reductions at ca. 1.8, 1.26, and 0.9 Ma. Estimates of MAP, with mean values of 664 mm for Shangchen ($n = 11$) and 709 mm for Duanjiapo ($n = 11$), exhibit a wide (>300 mm) range through the sequence. MAP at both locations declines abruptly after ca. 1.26 Ma.

3.5. Variability Changes of Proxies

Changes in variability of SUS, BC, and $\delta^{13}\text{C}_{\text{TOC}}$ are represented by the moving standard deviations of the original data (see details of data processing in Text S2 in Supporting Information S1) and are similar across the three proxies and are generally at low levels before ~ 1.28 Ma (the beginning of S15; Figures 2h–2k). Much more substantial peaks occur during $\sim 1.26\text{--}0.9$ Ma, that is, the early MPT.

4. Discussion

4.1. Climate, Vegetation Conditions, and Hominin Occupation Through the Pleistocene

Our data show that, between 2.1 and 0.6 Ma, environmental conditions at Shangchen can be divided into four distinct stages: 2.1–1.8, 1.8–1.26, 1.26–0.9, and 0.9–0.6 Ma (detailed in Text S3 in Supporting Information S1). During 2.1–1.8 Ma, variability changes of proxies (Vc-proxies) are consistently small (Figures 2i–2k), suggesting that climate and vegetation conditions varied little. From 1.8 to 1.26 Ma, values of all proxies remain relatively stable, with no prominent peaks (Figures 2i–2k). Both %BC and MAP (Figure 3a) indicate that the climate was still relatively wet during this period, and the contribution of C_4 herbaceous taxa to vegetation declined in favor of an increase in C_3 plants (Figure 3f). The period between 1.26 and 0.9 Ma exhibits pronounced peaks in climate and vegetation variability, as shown by Vc-proxies (Figures 2i–2k), and C_4 taxa exhibit a long-term expansion trend from ~ 1.26 Ma (Figure 3f). In addition, increasing BC concentrations and decreasing br-GDGTs-derived MAP indicate changes in the fire regime and an aridification trend since the beginning of MPT (~ 1.26 Ma;

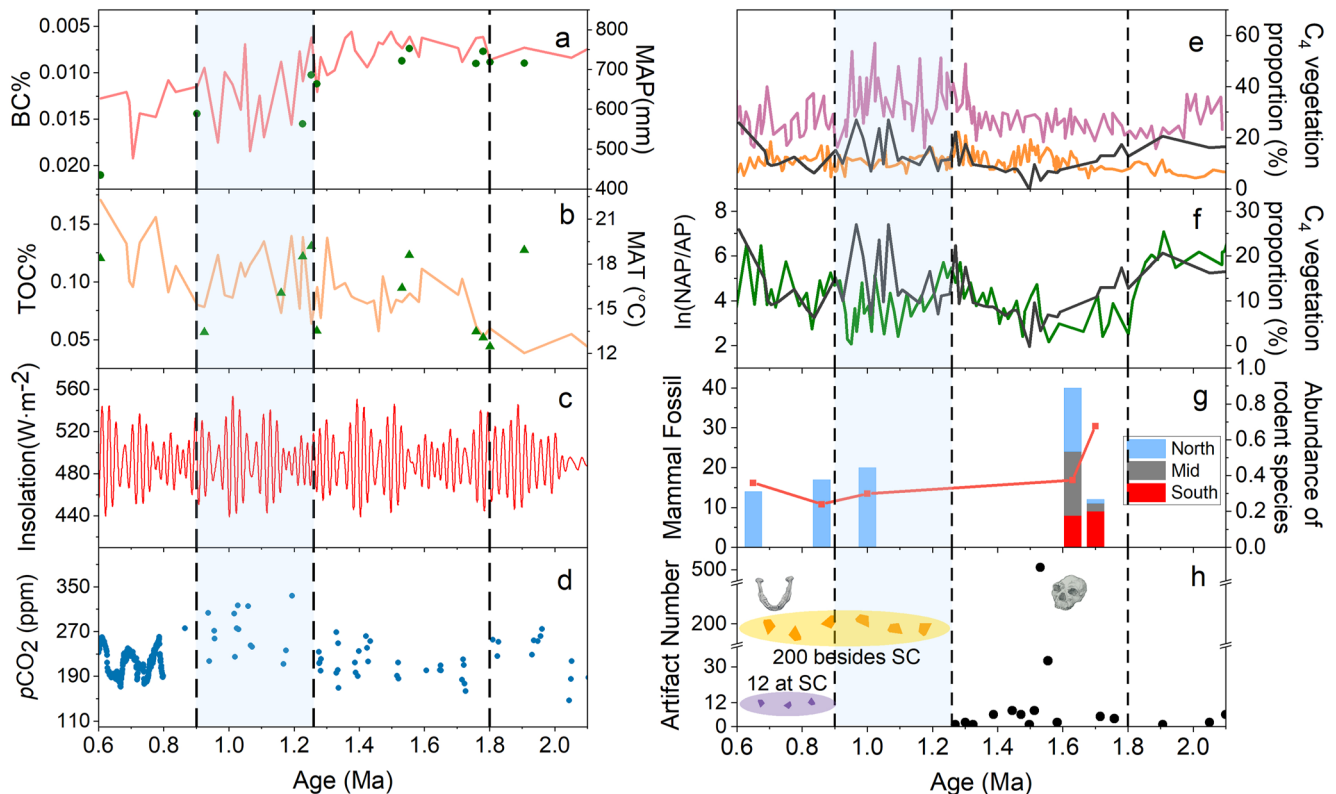


Figure 3. Temporal trends in climate, vegetation and artifacts in Lantian. (a) Black carbon (BC%; pink line) and mean annual precipitation (MAP; green dots) and (b) total organic carbon (TOC%; orange line) and mean annual temperature (MAT; green triangles) at Shangchen; (c) summer insolation at 34°N (Berger & Loutre, 1991); (d) Median levels of $p\text{CO}_2$ distributions (2.1–0.8 Ma; Da et al., 2019) and ice core CO_2 record (0.8–0.6 Ma; Lüthi et al., 2008); (e) C_4 vegetation proportions around Lantian. Black line = Shangchen, orange line = Yanyu estimated by data in Sun et al. (2012), purple line = Duanjiapo estimated by data in An et al. (2005); (f) green line = $\ln(\text{NAP/AP})$ (the natural logarithm of Non Arboreal Pollen/Arboreal Pollen ratio) at Chaona in the central Chinese Loess Plateau (Wu et al., 2007), black line = C_4 vegetation proportion at Shangchen; (g) classification of mammal fossil species and abundance of rodent species to total mammal fossil species in Lantian area; (h) numbers of artifacts and fossils of *Homo erectus* in Lantian area (Huang, 1983; Zhu et al., 2015). Purple ellipse represents artifacts at Shangchen during 1.26–0.6 Ma. Yellow ellipse represents artifacts at other sites in Lantian area during the middle Pleistocene (S. Wang et al., 2014). Black dots represent artifacts records during 2.1–1.26 Ma in Lantian area. Black dashed lines represent 0.9, 1.26, and 1.8 Ma.

Figure 3a), which, possibly enhanced by shifts in seasonality (e.g., Jones et al., 2022), favored a more open vegetation environment with a higher proportion of C_4 plants (Zhou et al., 2014, 2017). The greater amplitude of glacial-interglacial variations during this early MPT phase is evident in grain size, C_3/C_4 ratios and, indeed, in vegetation records from elsewhere on the CLP (An et al., 2005; Y. Sun et al., 2019). Reduced sensitivity of monsoonal temperature and precipitation to insolation forcing (Figure 3c), and changes in astronomical forcing under different ice/ CO_2 boundary conditions (Figures 2g and 3d), may have driven variability changes of climate and vegetation on the CLP during the early MPT (Y. Sun et al., 2019). During the 0.9–0.6 Ma, low values of SUS, MAT, and MAP, and higher BC% indicate weaker summer monsoon and generally similar cool and arid climate as the previous period, while lower $\delta^{13}\text{C}_{\text{TOC}}$ values suggest an increased prominence of C_3 taxa in the vegetation, which was dominated by C_3 shrubs as evidenced by the pollen record from Chaona (Wu et al., 2007).

A relationship between changes in climatic and environmental proxies, Vc-proxies, faunal assemblage and the number of artifacts is evident in the record (Figure 2 and Supporting Information S1). In all, nine stone tools were found in three loess/paleosol layers (S26, L27, and S27) at Shangchen between 2.1 and 1.8 Ma (Zhu et al., 2018). However, during 1.8–1.26 Ma, 79 stone tools were found and the mean number of artifacts over time in this period is greater than during 2.1–1.8 Ma (Zhu et al., 2018). Evidence for the more prominent presence of hominins during 1.8–1.26 Ma is associated with a similarly wet and warmer environment (high MAP and MAT values in Figures 2e and 2f). Faunal remains of several taxa typically associated with a more southerly distribution, including *Ailuropoda melanoleuca fovealis*, *Stegodon orientalis*, *Elaphodus cephalophus*, were recovered from a site nearby Gongwangling, along with a cranium identified as *H. erectus* (layer S23, ~1.63–1.62 Ma; Figure 3h; Zhu

et al., 2015). These taxa are restricted to areas to the south of the modern Qinling Mountains, indicating that the study area was warmer and wetter at that time than it is at present, and that more luxuriant vegetation was able to support large mammals and early humans (Xue et al., 2006). Moreover, the conspicuously high number of artifacts found in layer S22 (~1.57–1.54 Ma) at Shangchen is similar in age to that of the Gongwangling cranium (Zhu et al., 2015; Figures 2h and 3h). Before ~1.28 Ma (the beginning of S15), Vc-proxies suggest relatively low climate and environmental variability, while the frequency of artifacts in loess/paleosol layers below layer S15 signifies ongoing hominin occupation, albeit discontinuous. The occurrence of artifacts that point to local occupation by early humans abruptly ceases between layer L15 (~1.26–1.24 Ma) and layer S8 (~0.87–0.82 Ma) and there is an absence of faunal remains between ca. 1.26 Ma and ca. 1.0 Ma (Figures 2h and 3g). This is in keeping with evidence from Vc-proxies, which show unprecedented peaks at the L15/S15 boundary (~1.26 Ma; Figures 2i–2k). Shortly after this strikingly rapid shift in climate and vegetation conditions, the lithics record at Shangchen and the large mammal fossil record around Lantian is truncated. The absence of lithics at Shangchen is accompanied by substantial increases in the frequency and magnitude changes in climate and vegetation, as indicated by recurrent peaks in Vc-proxies between 1.26 and 0.9 Ma that continued through the phase (Figures 2i–2k). Furthermore, after 0.9 Ma, the Chenjiawo fauna that was discovered along with a *H. erectus* mandible (~0.65 Ma) exhibits distinct northern temperate affiliations (Xue et al., 2006; Figures 3g and 3h). The occurrence of 12 artifacts at Shangchen during 0.9–0.6 Ma, a markedly lower concentration than before 1.26 Ma (Zhu et al., 2018), is also noteworthy. According to evidence indicated by MAT, MAP, and %BC, the shift in faunal assemblage from one dominated by taxa associated with areas well to the south of the study area to those typical of temperate areas to the north, as well as declining hominin activities after ~1.26 Ma at Shangchen, is related to a long-term cooling and aridification trend since the onset of the early MPT (Figures 3a and 3b). We conclude here that greater environmental (climate-vegetation) variability and continuous aridity during the early MPT led to the Shangchen occupants migrating out of the region and/or becoming locally extinct.

4.2. Early Human Settlement in the Context of Local Vegetation and Water Conditions Across the Chinese Loess Plateau

Based on existing $\delta^{13}\text{C}_{\text{TOC}}$ records from sections around Lishan Mountain, including Shangchen (this study) and Yanyu (J. Sun et al., 2012), estimated variations in relative abundances of C_4 taxa exhibit notable similarities. The mean values of -25.4‰ and -25.5‰ , respectively, suggest that C_4 plants constituted approximately 12% of the vegetation biomass during the early to middle Pleistocene. In contrast, the average $\delta^{13}\text{C}_{\text{TOC}}$ derived from Duanjiapo on the BLT (An et al., 2005), is consistently about 3‰ more enriched, suggesting a 20% greater contribution of C_4 taxa (Figure 3e). The proportion of C_4 plants in vegetation may be poorly related to the relative abundance of non-arboreal pollen due to production biases (Ficken et al., 2002). However, variations in the contribution of C_4 taxa to vegetation recorded at Shangchen correlate with the rhythm of fluctuations in the ratio of non-arboreal to arboreal pollen (i.e., $\ln(\text{NAP/AP})$) in loess sediments from Chaona in the central CLP (Figure 3f; Wu et al., 2007), supporting the view that a decrease in the proportion of C_4 represents an increase in tree cover (Cerling et al., 2011; Osborne, 2007; Zhou et al., 2014). The sedimentary evidence thus indicates less woodland cover at Duanjiapo compared with Shangchen (Figure 3e). This is despite similar MAP and MAT reconstructions for the two sites, with the apparent incongruity possibly due to the ecological effects of local differences in edaphic conditions (Compilation Committee of Local Chronicles of Shaanxi Province, 2000; Mertes et al., 1995). The stepwise uplift of Lishan Mountain since the Late-Pliocene (X. Gao & Wang, 1990), resulted in the formation of five river terrace levels (Lei & Qu, 1992). Paleolithic sites of Shangchen as well as Gongwangling around Lishan Mountain, were situated closer to Bahe river than Duanjiapo (Figure S6 in Supporting Information S1). Accordingly, the riparian corridor around Lishan Mountain, was characterized by more trees, large predators and access to water and stones, and was therefore able to provide hominins with shelter and moreover, access to additional food resources and raw materials for stone tools. Meanwhile, based on paleotopography and the mean rate of river incision (Lei & Qu, 1992), the elevational difference between BLT and the Bahe River, separated by a steep escarpment, would have exceeded 100 m and therefore reduced access to water from Bahe river and any bedrock or stone for tool manufacture (Figure S6 in Supporting Information S1). Moreover, due to the relatively subdued topography, coupled with the permeable nature of the loess substrate, surface water bodies are rare on the BLT, restricting access to reliable water supplies and thereby preventing early hominins from occupying the locality. Therefore, local environmental conditions were most likely to be suitable for early hominin occupation at Shangchen, at least until the MPT.

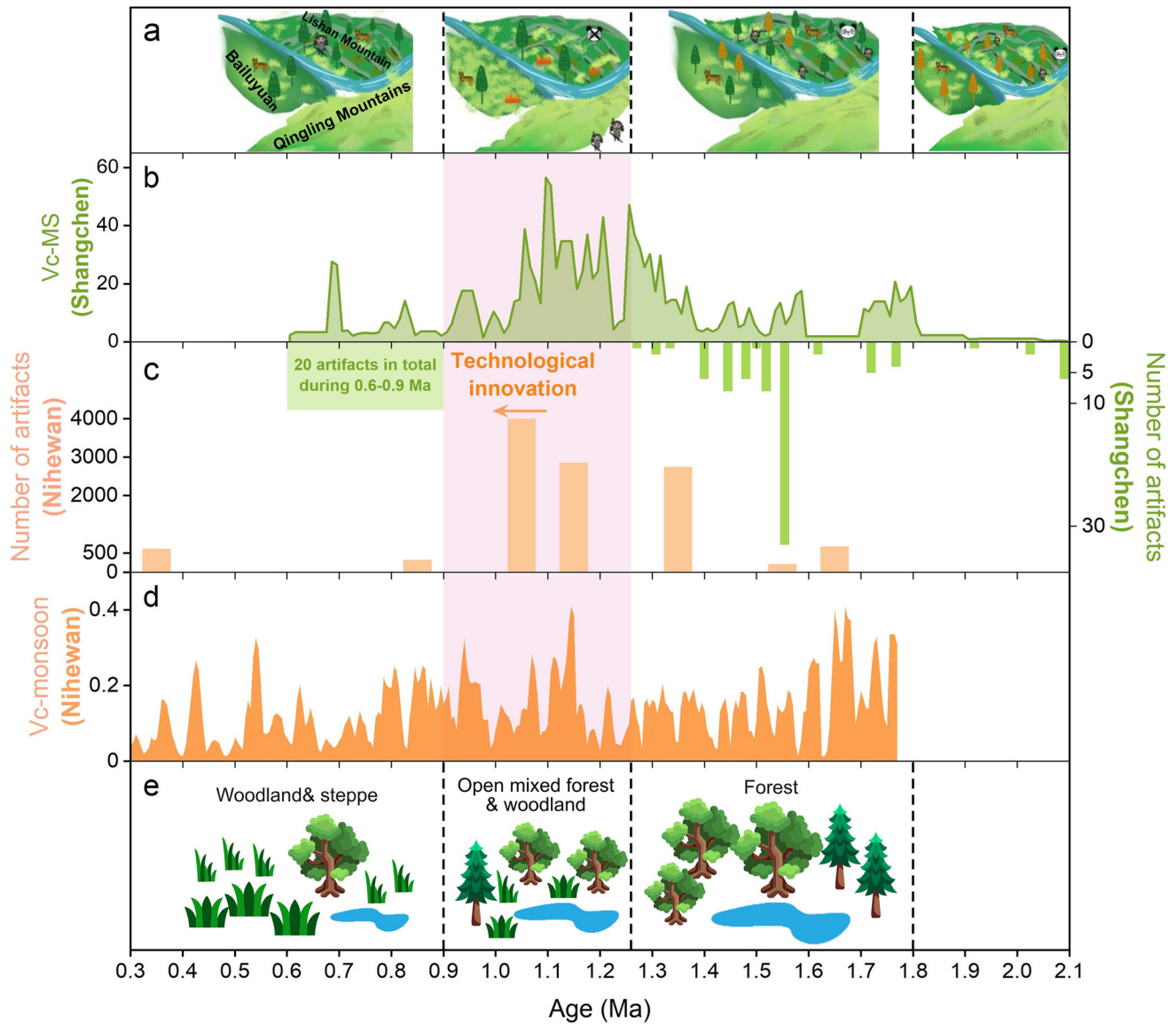


Figure 4. Relationships between climate variability, local environment and hominin activities at Shangchen and Nihewan. (a) Diagram of local environment during different periods at Shangchen (this paper). The panda icon is used to represent the subtropical fauna normally found south of the Qinling Mountains. (b) Vc-SUS at Shangchen (this paper). (c) Timeseries of number of artifacts found at Shangchen (green; Zhu et al., 2018) and Nihewan (orange; Yang et al., 2021). The arrow represents the technological innovation of human tool use during ~ 1.1 – 1.0 Ma at Nihewan (Yang et al., 2021). (d) Vc-monsoon derived by Nihewan monsoon index from Ao et al. (2012). Light purple boxes in panels (b–d) represent the mid-Pleistocene climate transition during 1.26 – 0.9 Ma. (e) Diagram of local environment during different periods at Nihewan (revised from Yang et al. (2021)). Dashed lines represent 0.9 , 1.26 , and 1.8 Ma. The icons are obtained from www.flaticon.com.

The situation at Shangchen during the early MPT contrasts with the contemporaneous sequence of events in the Qinling mountains to the south. Lithic artifacts initially appeared in the L15 layer (~ 1.26 Ma) at Longgangsi in the southern Qinling Mountains (X. Sun et al., 2018) simultaneously with the truncation of the artifacts record at Shangchen. The lithics record then continued during ~ 1.2 – 0.7 Ma at Longgangsi (X. Sun et al., 2018), implying that ancient humans migrated to wetter and warmer areas to the south of the Qinling Mountains. Moreover, toolmaking skills and numbers and varieties of stone tools found at occupation sites in the Nihewan Basin, at the northeast margin of the CLP, are reported to have increased during the early MPT, consistent with the adoption of new technologies, and suggesting that early humans were adaptively flexible in responding to climate-driven changes (Figures 4c–4e; Yang et al., 2020, 2021). The contraction of the lake at Nihewan as a result of increased aridity in the early stages of the MPT provided a suitable living space for hominins in the form of an exposed open lacustrine basin terrace with access to water and food resources (Figure 4e; Yang et al., 2021). Comparison

with records at Nihewan indicates that large-scale climate oscillations during MPT induced disparate hominin responses due to distinctive local environmental conditions.

5. Conclusions

We analyzed SUS, TOC, BC, and $\delta^{13}\text{C}_{\text{TOC}}$ through a ~ 1.5 Ma-long loess-paleosol sequence sampled near the Shangchen Paleolithic sites as well as br-GDGTs from Shangchen and Duanjiapo, on the southeastern flank of the CLP. The results suggest that the area was dominated by C_3 vegetation, presumably including trees, throughout the record, from 2.1 to 0.6 Ma. C_4 herbaceous vegetation became more prominent at Shangchen, coincident with the higher climate variability driven by the MPT between 1.26 and 0.9 Ma.

Evidence in the form of variations in environmental proxies, the distribution of stone tools in loess-paleosol strata, and the remains of fauna suggests that early humans appear to have preferred sites that were characterized by being environmentally stable, wooded (C_3 -dominated) with incised topography and relatively easy access to surface water over wide, exposed and resource/refuge-poor loess tableland locations in the southeast of the CLP. These early human occupants of the CLP appear to have relocated to more hospitable locations during periods of strong recurrent environmental variability associated with, in particular, the MPT.

Data Availability Statement

The SUS, TOC%, BC%, $\delta^{13}\text{C}_{\text{TOC}}$, and br-GDGTs based data used for paleoenvironments reconstruction in the study are available at Mendeley data (Zhou et al., 2023).

Acknowledgments

We thank Zhaoyu Zhu, Yi Wu for sampling, Hongxuan Lu for br-GDGTs discussion, Wentao Ma, Zhongfang Liu for discussion on data processing, Huayu Lu, Xuefeng Sun, Yige Zhang, Junfeng Ji, Jaiwei Da, and Min-Te Chen for reading a previous draft of this manuscript. This study was funded by Major Research Plan of the National Natural Science Foundation of China (Grand 41991323), the National Natural Science Foundation of China (41977378 and 41977379), the Guangzhou Institute of Geochemistry, Chinese Academy of Sciences (Y834019001).

References

- An, Z., & Ho, C. (1989). New magnetostratigraphic Dates of Lantian *Homo erectus*. *Quaternary Research*, 32(2), 213–221. [https://doi.org/10.1016/0033-5894\(89\)90077-X](https://doi.org/10.1016/0033-5894(89)90077-X)
- An, Z., Huang, Y., Liu, W., Guo, Z., Clemens, S., Li, L., et al. (2005). Multiple expansions of C_4 plant biomass in East Asia since 7 Ma coupled with strengthened monsoon circulation. *Geology*, 33(9), 705. <https://doi.org/10.1130/G21423.1>
- Ao, H., Dekkers, M. J., Xiao, G., Yang, X., Qin, L., Liu, X., et al. (2012). Different orbital rhythms in the Asian summer monsoon records from North and South China during the Pleistocene. *Global and Planetary Change*, 80–81, 51–60. <https://doi.org/10.1016/j.gloplacha.2011.09.012>
- Berger, A., & Loutre, M. F. (1991). Insolation values for the climate of the last 10 million years. *Quaternary Science Reviews*, 10(4), 297–317. [https://doi.org/10.1016/0277-3791\(91\)90033-Q](https://doi.org/10.1016/0277-3791(91)90033-Q)
- Bird, M. I., Wynn, J. G., Saiz, G., Wurster, C. M., & McBeath, A. (2015). The pyrogenic carbon cycle. *Annual Review of Earth and Planetary Sciences*, 43(1), 273–298. <https://doi.org/10.1146/annurev-earth-060614-105038>
- Blumenthal, S. A., Levin, N. E., Brown, F. H., Brugal, J.-P., Chrzt, K. L., Harris, J. M., et al. (2017). Aridity and hominin environments. *Proceedings of the National Academy of Sciences*, 114(28), 7331–7336. <https://doi.org/10.1073/pnas.1700597114>
- Cerling, T. E., Wynn, J. G., Andanje, S. A., Bird, M. I., Korir, D. K., Levin, N. E., et al. (2011). Woody cover and hominin environments in the past 6 million years. *Nature*, 476(7358), 51–56. <https://doi.org/10.1038/nature10306>
- Chen, F., Rao, Z., Jiawu, Z., Ming, J., & Jianying, M. (2006). Variations of organic carbon isotopic composition and its environmental significance during the last glacial on western Chinese Loess Plateau. *Chinese Science Bulletin*, 51(13), 1593–1602. <https://doi.org/10.1007/s11434-006-2003-6>
- Compilation Committee of Local Chronicles of Shaanxi Province. (2000). The Natural Environment of the Guanzhong plain basin region. In *Geographical chronicle of Shaanxi Province* (Ch. 16, Sec. 3). Shanxi People's Press.
- Da, J., Zhang, Y. G., Li, G., Meng, X., & Ji, J. (2019). Low CO_2 levels of the entire Pleistocene epoch. *Nature Communications*, 10(1), 4342. <https://doi.org/10.1038/s41467-019-12357-5>
- deMenocal, P. B. (2011). Climate and human evolution. *Science*, 331(6017), 540–542. <https://doi.org/10.1126/science.1190683>
- Ding, Z., Derbyshire, E., Yang, S., Yu, Z., Xiong, S., & Liu, T. (2002). Stacked 2.6-Ma grain size record from the Chinese loess based on five sections and correlation with the deep-sea $\delta^{18}\text{O}$ record. *Paleoceanography*, 17(3), 5–1–5–21. <https://doi.org/10.1029/2001PA000725>
- Ficken, K. J., Wooller, M. J., Swain, D. L., Street-Perrott, F. A., & Eglinton, G. (2002). Reconstruction of a subalpine grass-dominated ecosystem, Lake Rutundu, Mount Kenya: A novel multi-proxy approach. *Palaeogeography, Palaeoclimatology, Palaeoecology*, 177(1–2), 137–149. [https://doi.org/10.1016/S0031-0182\(01\)00356-X](https://doi.org/10.1016/S0031-0182(01)00356-X)
- Gao, X., & Wang, H. (1990). The reason for the concentrated accumulation of Gongwangling fossils and the living environment of the Lantian hominins. *Relics and Museology*, 7, 27–31.
- Guo, Z., Ruddiman, W. F., Hao, Q., Wu, H., Qiao, Y., Zhu, R., et al. (2002). Onset of Asian desertification by 22 Myr ago inferred from loess deposits in China. *Nature*, 416(6877), 159–163. <https://doi.org/10.1038/416159a>
- Han, Y., An, Z., Marlon, J. R., Bradley, R. S., Zhan, C., Arimoto, R., et al. (2020). Asian inland wildfires driven by glacial–interglacial climate change. *Proceedings of the National Academy of Sciences*, 117(10), 5184–5189. <https://doi.org/10.1073/pnas.1822035117>
- Huang, C. (1983). Discovery of the paleolithic cultural site at Xishui Cave, Lantian, Shaanxi and its significance. *Chinese Science Bulletin*, 4, 241–244.
- Jones, M. W., Abatzoglou, J. T., Veraverbeke, S., Andela, N., Lasslop, G., Forkel, M., et al. (2022). Global and regional trends and drivers of fire under climate change. *Reviews of Geophysics*, 60(3), e2020RG000726. <https://doi.org/10.1029/2020RG000726>
- Lei, X., & Qu, H. (1992). The loess-paleosol sequences of the Bahe River terraces and their chronological significance. *Journal of Northwest University*, 22, 219–226.

- Lisiecki, L. E., & Raymo, M. E. (2005). A Pliocene-Pleistocene stack of 57 globally distributed benthic $\delta^{18}\text{O}$ records. *Paleoceanography*, 20(1), PA1003. <https://doi.org/10.1029/2004PA001071>
- Liu, W., Ning, Y., An, Z., Wu, Z., Lu, H., & Cao, Y. (2005). Carbon isotopic composition of modern soil and paleosol as a response to vegetation change on the Chinese Loess Plateau. *Science in China – Series D: Earth Sciences*, 48(1), 93–99. <https://doi.org/10.1360/02yd0148>
- Lüthi, D., Le Floch, M., Bereiter, B., Blunier, T., Barnola, J.-M., Siegenthaler, U., et al. (2008). High-resolution carbon dioxide concentration record 650,000–800,000 years before present. *Nature*, 453(7193), 379–382. <https://doi.org/10.1038/nature06949>
- Magill, C. R., Ashley, G. M., & Freeman, K. H. (2013a). Ecosystem variability and early human habitats in eastern Africa. *Proceedings of the National Academy of Sciences*, 110(4), 1167–1174. <https://doi.org/10.1073/pnas.1206276110>
- Magill, C. R., Ashley, G. M., & Freeman, K. H. (2013b). Water, plants, and early human habitats in eastern Africa. *Proceedings of the National Academy of Sciences*, 110(4), 1175–1180. <https://doi.org/10.1073/pnas.1209405109>
- Maslin, M. A., Brierley, C. M., Milner, A. M., Shultz, S., Trauth, M. H., & Wilson, K. E. (2014). East African climate pulses and early human evolution. *Quaternary Science Reviews*, 101, 1–17. <https://doi.org/10.1016/j.quascirev.2014.06.012>
- Mertes, L. A., Daniel, D. L., Melack, J. M., Nelson, B., Martinelli, L. A., & Forsberg, B. R. (1995). Spatial patterns of hydrology, geomorphology, and vegetation on the floodplain of the Amazon River in Brazil from a remote sensing perspective. *Geomorphology*, 13(1–4), 215–232. [https://doi.org/10.1016/0169-555X\(95\)00038-7](https://doi.org/10.1016/0169-555X(95)00038-7)
- Osborne, C. P. (2007). Atmosphere, ecology and evolution: What drove the Miocene expansion of C_4 grasslands? *Journal of Ecology*, 96(1), 071204085531001. <https://doi.org/10.1111/j.1365-2745.2007.01323.x>
- Owen, R. B., Muiruri, V. M., Lowenstein, T. K., Renaut, R. W., Rabideaux, N., Luo, S., et al. (2018). Progressive aridification in East Africa over the last half million years and implications for human evolution. *Proceedings of the National Academy of Sciences*, 115(44), 11174–11179. <https://doi.org/10.1073/pnas.1801357115>
- Peterse, F., Martínez-García, A., Zhou, B., Beets, C. J., Prins, M. A., Zheng, H., & Eglinton, T. I. (2014). Molecular records of continental air temperature and monsoon precipitation variability in East Asia spanning the past 130,000 years. *Quaternary Science Reviews*, 83, 76–82. <https://doi.org/10.1016/j.quascirev.2013.11.001>
- Potts, R. (1996). Evolution and climate variability. *Science*, 273(5277), 922–923. <https://doi.org/10.1126/science.273.5277.922>
- Potts, R., Dommoin, R., Moerman, J. W., Behrensmeier, A. K., Deino, A. L., Riedl, S., et al. (2020). Increased ecological resource variability during a critical transition in hominin evolution. *Science Advances*, 6(43), eabc8975. <https://doi.org/10.1126/sciadv.abc8975>
- Shen, G., Wang, Y., Tu, H., Tong, H., Wu, Z., Kuman, K., et al. (2020). Isochron $^{26}\text{Al}/^{10}\text{Be}$ burial dating of Xihoudu: Evidence for the earliest human settlement in northern China. *L'Anthropologie*, 124(5), 102790. <https://doi.org/10.1016/j.anthro.2020.102790>
- Song, Y., Fang, X., King, J. W., Li, J., Naoto, I., & An, Z. (2014). Magnetic parameter variations in the Chaona loess/paleosol sequences in the central Chinese Loess Plateau, and their significance for the middle Pleistocene climate transition. *Quaternary Research*, 81(3), 433–444. <https://doi.org/10.1016/j.yqres.2013.10.002>
- Sun, J., Lü, T., Zhang, Z., Wang, X., & Liu, W. (2012). Stepwise expansions of C_4 biomass and enhanced seasonal precipitation and regional aridity during the Quaternary on the southern Chinese Loess Plateau. *Quaternary Science Reviews*, 34, 57–65. <https://doi.org/10.1016/j.quascirev.2011.12.007>
- Sun, X., Lu, H., Wang, S., Xu, X., Zeng, Q., Lu, X., et al. (2018). Hominin distribution in glacial-interglacial environmental changes in the Qinling Mountains range, central China. *Quaternary Science Reviews*, 198, 37–55. <https://doi.org/10.1016/j.quascirev.2018.08.012>
- Sun, Y., Yin, Q., Crucifix, M., Clemens, S. C., Araya-Melo, P., Liu, W., et al. (2019). Diverse manifestations of the mid-Pleistocene climate transition. *Nature Communications*, 10(1), 1–11. <https://doi.org/10.1038/s41467-018-08257-9>
- Tu, H., Shen, G., Granger, D., Yang, X., & Lai, Z. (2017). Isochron $^{26}\text{Al}/^{10}\text{Be}$ burial dating of the Lantian hominin site at Gongwangling in north-western China. *Quaternary Geochronology*, 41, 174–179. <https://doi.org/10.1016/j.quageo.2017.04.004>
- Wang, G., Feng, X., Han, J., Zhou, L., Tan, W., & Su, F. (2008). Paleovegetation reconstruction using $\delta^{13}\text{C}$ of Soil Organic Matter. *Biogeosciences*, 5(5), 1325–1337. <https://doi.org/10.5194/bg-5-1325-2008>
- Wang, S., Lu, H., Zhang, H., Sun, X., Yi, S., Chen, Y., et al. (2014). Newly discovered Palaeolithic artefacts from loess deposits and their ages in Lantian, central China. *Chinese Science Bulletin*, 59(7), 651–661. <https://doi.org/10.1007/s11434-013-0105-5>
- Weijers, J. W. H., Schouten, S., van den Donker, J. C., Hopmans, E. C., & Sinninghe Damsté, J. S. (2007). Environmental controls on bacterial tetraether membrane lipid distribution in soils. *Geochimica et Cosmochimica Acta*, 71(3), 703–713. <https://doi.org/10.1016/j.gca.2006.10.003>
- Willeit, M., Ganopolski, A., Calov, R., & Brovkin, V. (2019). Mid-Pleistocene transition in glacial cycles explained by declining CO_2 and regolith removal. *Science Advances*, 5(4), eaav7337. <https://doi.org/10.1126/sciadv.aav7337>
- Wu, F., Fang, X., Ma, Y., Herrmann, M., Mosbrugger, V., An, Z., & Miao, Y. (2007). Plio–Quaternary stepwise drying of Asia: Evidence from a 3-Ma pollen record from the Chinese Loess Plateau. *Earth and Planetary Science Letters*, 257(1–2), 160–169. <https://doi.org/10.1016/j.epsl.2007.02.029>
- Xue, X., Zhang, Y., & Yue, L. (2006). Paleoenvironments indicated by the fossil mammalian assemblages from red clay-loess sequence in the Chinese Loess Plateau since 8.0 Ma B.P. *Science in China, Series D*, 49(5), 518–530. <https://doi.org/10.1007/s11430-006-0518-y>
- Yang, S., Ding, Z., Li, Y., Wang, X., Jiang, W., & Huang, X. (2015). Warming-induced northwestward migration of the East Asian monsoon rain belt from the Last Glacial Maximum to the mid-Holocene. *Proceedings of the National Academy of Sciences*, 112(43), 13178–13183. <https://doi.org/10.1073/pnas.1504688112>
- Yang, S., Wang, F., Xie, F., Yue, J., Deng, C., Zhu, R., & Petraglia, M. D. (2021). Technological innovations at the onset of the mid-Pleistocene climate transition in high-latitude East Asia. *National Science Review*, 8(1), nwaa053. <https://doi.org/10.1093/nsr/nwaa053>
- Yang, S., Yue, J., Zhou, X., Storozum, M., Huan, F., Deng, C., & Petraglia, M. D. (2020). Hominin site distributions and behaviours across the mid-Pleistocene climate transition in China. *Quaternary Science Reviews*, 248, 106614. <https://doi.org/10.1016/j.quascirev.2020.106614>
- Zhou, B., Bird, M., Zheng, H., Zhang, E., Wurster, C. M., Xie, L., & Taylor, D. (2017). New sedimentary evidence reveals a unique history of C_4 biomass in continental East Asia since the early Miocene. *Scientific Reports*, 7(1), 170. <https://doi.org/10.1038/s41598-017-00285-7>
- Zhou, B., Shen, C., Sun, W., Bird, M., Ma, W., Taylor, D., et al. (2014). Late Pliocene–Pleistocene expansion of C_4 vegetation in semiarid East Asia linked to increased burning. *Geology*, 42(12), 1067–1070. <https://doi.org/10.1130/G36110.1>
- Zhou, B., Shen, C., Sun, W., Zheng, H., Yang, Y., Sun, Y., & An, Z. (2007). Elemental carbon record of paleofire history on the Chinese Loess Plateau during the last 420 ka and its response to environmental and climate changes. *Palaeogeography, Palaeoclimatology, Palaeoecology*, 252(3–4), 617–625. <https://doi.org/10.1016/j.palaeo.2007.05.014>
- Zhou, B., Wali, G., Peterse, F., & Bird, M. I. (2016). Organic carbon isotope and molecular fossil records of vegetation evolution in central Loess Plateau since 450 kyr. *Science China Earth Sciences*, 59(6), 1206–1215. <https://doi.org/10.1007/s11430-016-5276-x>
- Zhou, B., Wang, Z., Xu, X., & Pang, Y. (2023). Bulk, molecular and isotopic data from 2.1 to 0.6 Ma on southeastern Loess Plateau (version 1) [Dataset]. Mendeley Data. <https://doi.org/10.17632/km25ccvpz5.1>

- Zhu, Z., Dennell, R., Huang, W., Wu, Y., Qiu, S., Yang, S., et al. (2018). Hominin occupation of the Chinese Loess Plateau since about 2.1 million years ago. *Nature*, 559(7715), 608–612. <https://doi.org/10.1038/s41586-018-0299-4>
- Zhu, Z., Dennell, R., Huang, W., Wu, Y., Rao, Z., Qiu, S., et al. (2015). New dating of the *Homo erectus* cranium from Lantian (Gongwangling), China. *Journal of Human Evolution*, 78, 144–157. <https://doi.org/10.1016/j.jhevol.2014.10.001>

References From the Supporting Information

- De Jonge, C., Hopmans, E. C., Zell, C. I., Kim, J. H., Schouten, S., & Sinninghe Damsté, J. S. (2014). Occurrence and abundance of 6-methyl branched glycerol dialkyl glycerol tetraethers in soils: Implications for palaeoclimate reconstruction. *Geochimica et Cosmochimica Acta*, 141, 97–112. <https://doi.org/10.1016/j.gca.2014.06.013>
- Kukla, G., Heller, F., Ming, L., Chun, X., Sheng, L., & Sheng, A. (1988). Pleistocene climates in China dated by magnetic susceptibility. *Geology*, 16(9), 811. [https://doi.org/10.1130/0091-7613\(1988\)016<0811:PCICDB>2.3.CO;2](https://doi.org/10.1130/0091-7613(1988)016<0811:PCICDB>2.3.CO;2)
- LaRiviere, J. P., Ravelo, A. C., Crimmins, A., Dekens, P. S., Ford, H. L., Lyle, M., & Wara, M. W. (2012). Late Miocene decoupling of oceanic warmth and atmospheric carbon dioxide forcing. *Nature*, 486(7401), 97–100. <https://doi.org/10.1038/nature11200>
- Levin, N. E., Brown, F. H., Behrensmeyer, A. K., Bobe, R., & Cerling, T. E. (2011). Paleosol carbonates from the Omo Group: Isotopic records of local and regional environmental change in East Africa. *Palaeogeography, Palaeoclimatology, Palaeoecology*, 307(1–4), 75–89. <https://doi.org/10.1016/j.palaeo.2011.04.026>
- Liu, Z., Shao, M., & Wang, Y. (2013). Large-scale spatial interpolation of soil pH across the Loess Plateau, China. *Environmental Earth Sciences*, 69(8), 2731–2741. <https://doi.org/10.1007/s12665-012-2095-z>
- Lu, H., Liu, W., Yang, H., Wang, H., Liu, Z., Leng, Q., et al. (2019). 800-kyr land temperature variations modulated by vegetation changes on Chinese Loess Plateau. *Nature Communications*, 10(1), 1958. <https://doi.org/10.1038/s41467-019-09978-1>
- Tu, H., Luo, L., Deng, C., Ou, Z., Lai, Z., Shen, G., et al. (2022). Isochron $^{26}\text{Al}/^{10}\text{Be}$ burial dating of the Xiashagou Fauna in the Nihewan Basin, northern China: Implications for biogeography and early hominin dispersals. *Quaternary Science Reviews*, 283, 107447. <https://doi.org/10.1016/j.quascirev.2022.107447>
- Wang, B., Zheng, H., Wang, P., & He, Z. (2013). The Cenozoic strata and depositional evolution of Weihe basin: Progresses and problems. *Advances in Earth Science*, 28, 1126–1135. <https://doi.org/10.11867/j.issn.1001-8166.2013.10.1126>
- Wang, G., Han, J., & Liu, D. (2003). The carbon isotope composition of C_3 herbaceous plants in loess area of northern China. *Science in China - Series D: Earth Sciences*, 46(10), 1069–1076. <https://doi.org/10.1007/BF02959402>
- Wang, G., Han, J., Zhou, L., Xiong, X., Tan, M., Wu, Z., & Peng, J. (2006). Carbon isotope ratios of C_4 plants in loess areas of North China. *Science in China, Series A D*, 49(1), 97–102. <https://doi.org/10.1007/s11430-004-5238-6>
- Wang, H., Liu, W., & Zhang, C. (2014). Dependence of the cyclization of branched tetraethers on soil moisture in alkaline soils from arid–subhumid China: Implications for palaeorainfall reconstructions on the Chinese Loess Plateau. *Biogeosciences*, 11(23), 6755–6768. <https://doi.org/10.5194/bg-11-6755-2014>
- Wu, Y., Qiu, S., Fu, S., Rao, Z., & Zhu, Z. (2018). Pleistocene climate change inferred from multi-proxy analyses of a loess–paleosol sequence in China. *Journal of Asian Earth Sciences*, 154, 428–434. <https://doi.org/10.1016/j.jseaes.2017.10.007>
- Zhang, L., Hay, W. W., Wang, C., & Gu, X. (2019). The evolution of latitudinal temperature gradients from the latest Cretaceous through the present. *Earth-Science Reviews*, 189, 147–158. <https://doi.org/10.1016/j.earscirev.2019.01.025>
- Zhang, M. (2003). *The evolutionary model of river terraces in the mid-tail of Wei He River* (Master's thesis). Northwest University.
- Zhao, Z., Granger, D., Zhang, M., Kong, X., Yang, S., Chen, Y., & Hu, E. (2016). A test of the isochron burial dating method on fluvial gravels within the Pulu volcanic sequence, West Kunlun Mountains, China. *Quaternary Geochronology*, 34, 75–80. <https://doi.org/10.1016/j.quageo.2016.04.003>